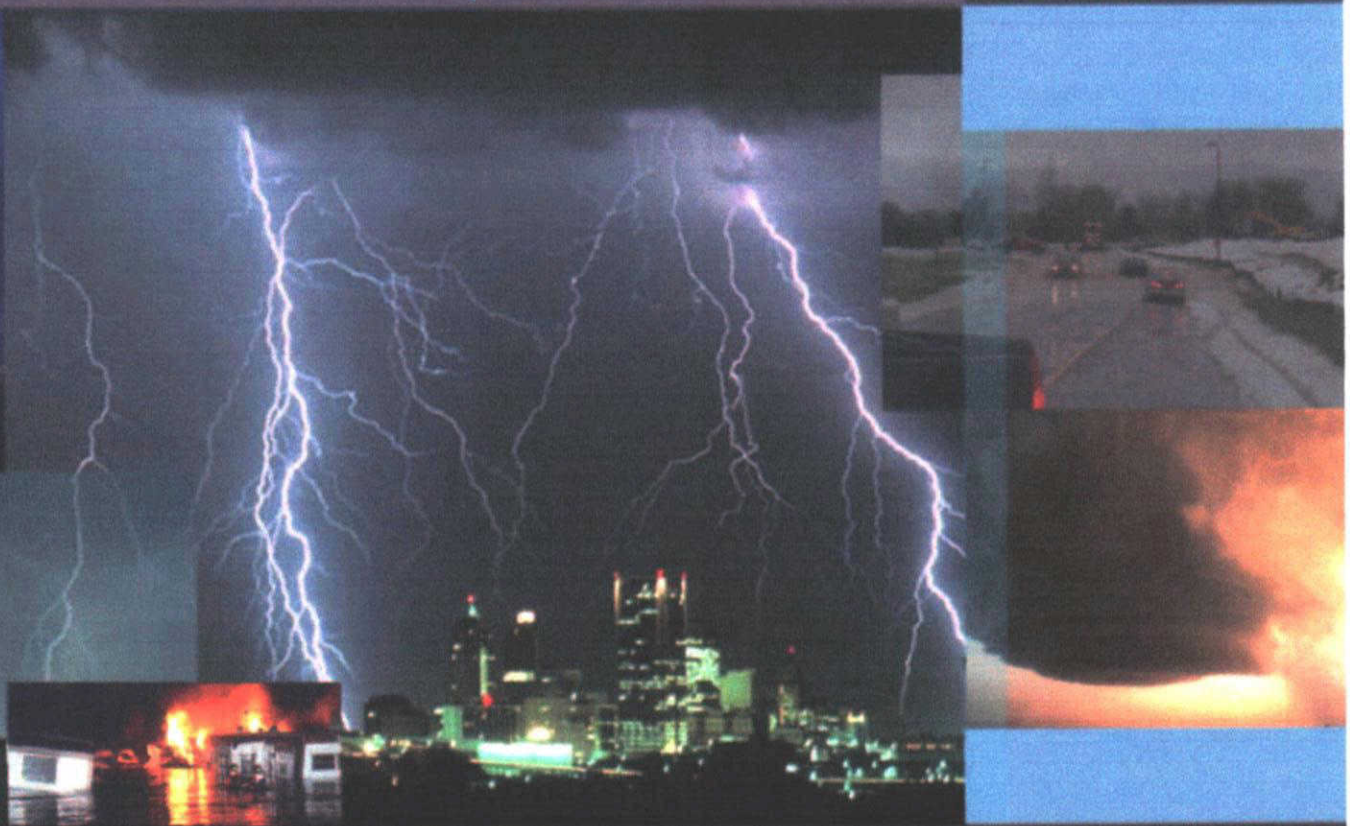


RADAR - RAINFALL RECONSTRUCTION OF THE SAGUACHE CREEK FLASH FLOOD of July 25, 1999



Prepared for
Colorado Water Conservation Board
Under PB PDA 0000000023

Completed by
HDR Hydro-Meteorological Services (HMS)

HDR

June 2001

TABLE OF CONTENTS

1.0	Introduction	Page 2
2.0	Synoptic Situation.....	Page 3
3.0	Data Sources, Analysis Techniques, and "Gridding" Procedures .	Page 6
3.1	Data Sources	Page 6
3.2	Use of Radar to Calculate Rainfall	Page 6
3.3	Saguache Creek Basin Rainfall Estimation Methodology	Page 8
3.4	Analysis of Radar Reflectivity and Rainfall	Page 10
4.0	Cloud to Ground Lightning Data	Page 13
4.1	CG Data and Topography	Page 13
4.2	CG Data and Radar Reflectivity	Page 16
4.3	CG Data and Grid Averaged Rainfall Rates	Page 17
5.0	Relationship of Rainfall to Topography	Page 17
6.0	Comparison of Runoff Derived and Radar Storm Rainfall	Page 20
7.0	Conclusions	Page 20

1.0 Introduction

On July 25th 1999, a portion of the Saguache Creek basin located northwest of the town of Saguache, Colorado experienced a localized yet intense period of rainfall. Heavy rainfall flooded Saguache Creek and its tributaries both north and south of Highway 114. The resultant flash flooding washed out of roads and bridges along with the inundation of crop and rangeland located in and along these flooded tributaries. The only rainfall observation associated with this storm was an unofficial report of approximately 7 inches of rain in three hours noted by an unidentified camper. (See **Figure 1**)

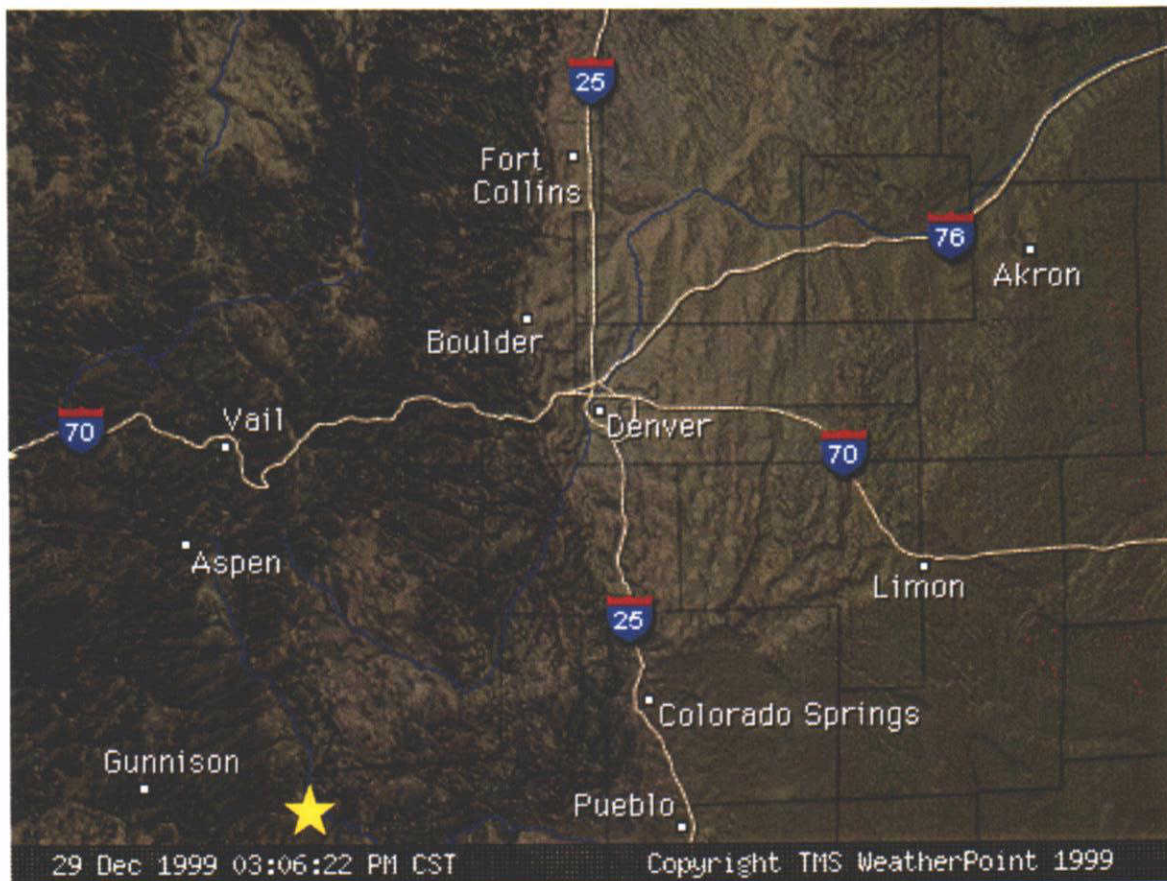


Figure 1
Location  of the Saguache Flash Flood of July 25, 1999

This flood event was brought about by an intense stationary thunderstorm complex that formed about mid-afternoon along the mountains to the northwest of Saguache, Colorado. This storm was but one of three impressive flash flooding events that occurred over western Colorado between July 25th and July 31st.

About the same time that the Saguache flash flood occurred, a deep mudslide closed I-70 just east of the Eisenhower Tunnel with up to 12-20 foot deep mud drifts across the highway. I-70 remained closed for almost 24 hours as crews struggled to remove the mudslide, rocks and debris from the interstate. Six days

later another intense mountain thunderstorm complex formed over the Dallas Divide and produced a monumental high country flash flood. These three events occurred during a prolonged, deep intrusion of monsoon moisture into the state.

The purpose of this report is to document the meteorological causes, reconstruct the estimated spatial coverage, temporal duration and rainfall depth of the thunderstorm complex that produced the flash flood. The general steps followed to acquire this information are:

1. A detailed meso-synoptic evaluation was completed of the weather causes of the storm using conventional surface and upper observations taken by the National Weather Service (NWS).
2. NWS WSR-88D Doppler radar observations from the Pueblo radar site were analyzed to determine the duration, location and depth of rainfall produced.
3. Cloud-to-ground lightning observations were obtained from the National Lightning Data Network and analyzed for the relationship to the rainfall production and aerial coverage of the storm.
4. Finally, the storm location and amounts as determined by radar were compared to the actual topography and an independent paleo-hydrological estimate.

2.0 Synoptic Situation

The large-scale atmospheric pattern in which the Saguache Creek flood occurred was very typical of conditions conducive for producing flash flooding in central Colorado Mountains. Flash floods in this area typically occur in the late June to mid-September time frame when large amounts of sub-tropical moisture are drawn up into Colorado via south to southwesterly flow in the lower-to-mid-levels of the atmosphere.

A brief examination of a regional satellite photo 1600 UTC (10:00AM) on July 25th, 1999 (**Figure 2**) shows three disturbances in this unstable sub-tropical flow:

1. The first disturbance (1) is located across central Nebraska and can be seen as the decaying meso-scale convective complex (MCC).
2. The second disturbance (2) is located along the northern Front Range and Continental Divide just to the west of Denver.
3. The third disturbance is located near Durango in southwestern Colorado. This third disturbance is the one associated with the Saguache flash flood.

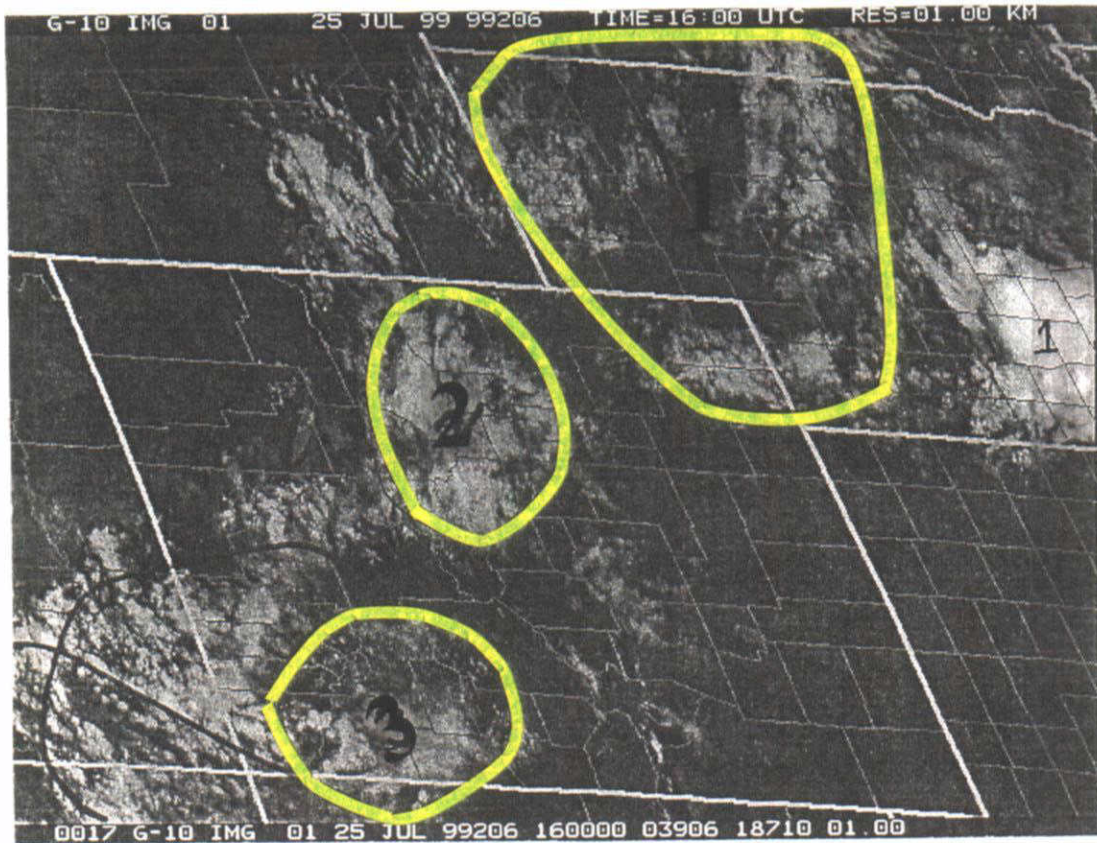


Figure 2
Sub-Tropical Disturbances Affected Colorado
In the Monsoon Flow

Surface dew points in central and western Colorado were generally in the upper 40s' and 50s (not shown) and the Surface to 500mb (~20,000 ft) Precipitable Water Indices (PWI) ranged from 0.92" at Albuquerque to 1.00" at Grand Junction at 600AM. These values were recomputed for the time of the flash flood and approached 1.15 inches. The values for both the dew points and the PWI are above average especially when one consider the elevation of many of the individual stations at which the observations were taken.

Further evidence for this 'moisture surge' of moisture, commonly referred to as the Mexican monsoon, can be found in the 700MB (~10,000ft) and 500MB (~19,000ft.) analyses (**Figures 3 and 4**) shown for 1200 UTC (6:00 AM MDT) on July 25th, 1999. The hatched area in these figures is indicative of very moist dew points at these levels (> +5°C at 700MB and > -15°C at 500MB). Excessive mid-level moisture is one of the key ingredients necessary for Colorado Mountain flash flooding. Dew points at 700MB of > 5C have a high likelihood of producing locally heavy rainfall. Note the narrow band of mid-level moisture flowing across the state. Clearly this "river of monsoon moisture" established the possible flooding locations by mid-morning.

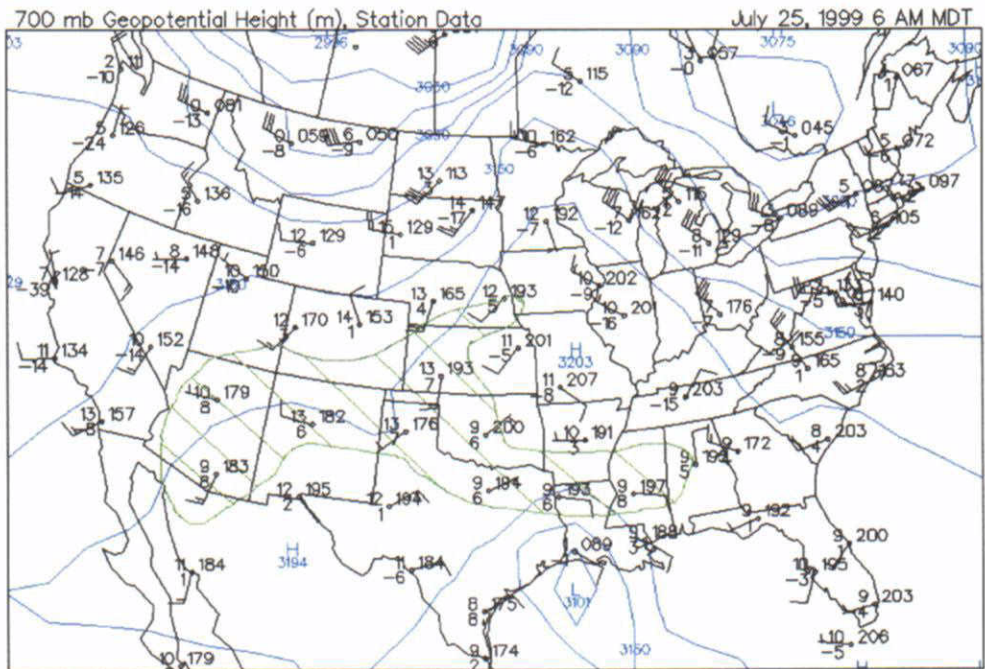


Figure 3
Analysis of 700 MB for 1200 UTC 25 July 1999

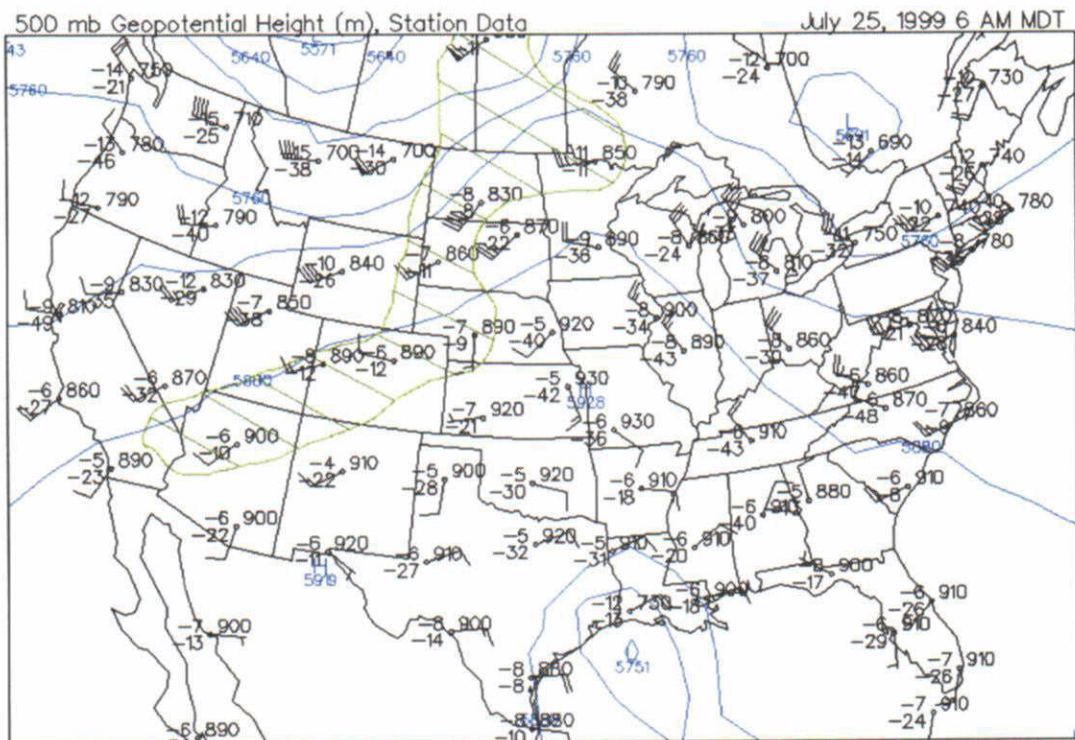


Figure 4
Analysis at 500 MB 1200 UTC 25 July 1999

When these two figures are superimposed (not shown) it indicates that the only region of the country in which both the 500 and 700 MB dew points are considered very moist is the Four Corners area that includes southern and southwestern Colorado. This indicates how deep moisture was present just to the southwest of the flooded area 7-10 hours prior to the flash flood.

Note that the mid-level wind direction was from the southwest and speeds were 10-15 mph. This wind direction is conducive to the formation of persistent thunderstorms on ridges that are oriented southwest to northeast. The low wind speeds are conducive to slow storm movement.

These two factors work together for the formation of either a large singular storm system anchored into topography by the cloud-layer winds or the development of successive storm formation that results in rainfall cores "training" over the same basin. In the case of the Saguache storm, the former event occurred as one large, persistent storm formed over the southwest facing mountain ridges just to the northwest of the town of Saguache.

3.0 Data Sources, Analysis Techniques, and "Gridding" Procedures

3.1 Data Sources

The procedures, techniques, and data utilized in the analysis of this event will be briefly described and further detailed in the following sections. Data utilized in this reconstruction includes, NEXRAD WSR-88D base reflectivity data from the National Weather Service Radar located near Pueblo, Co., upper air atmospheric soundings from Grand Junction and Denver, Co. along with Albuquerque, N.M., surface observations from numerous stations in Colorado and New Mexico, and cloud-to-ground lightning data from the National Lightning Detection Network (NLDN).

In order to better analyze some of the meteorological components of this event in a more efficient and accurate manner, a "grid" is established over the area in which the flash flood occurred. The size of one of the squares in the grid is coincidental with a pixel depicted in the NEXRAD data utilized in the rainfall analysis. Use of this grid is very helpful in deriving the rainfall totals, which will be described in more detail in the following section. In addition, this grid is extremely helpful in analyzing the cloud-to-ground lightning data and the relationship it has with the storm

3.2 Use of Radar to Calculate Storm Rainfall

The utilization of radar to estimate rainfall has been in use for over 30 years by meteorologists in both the government and the private sector. In general, most current radar-derived rainfall techniques rely on an assumed relationship between the strength of the

radar reflectivity and the intensity of the rainfall rate. This relationship is described by the equation (1) below:

$$(1) \quad Z = A R^b$$

Where, Z is the radar reflectivity in dBZ, A is an empirically derived co-efficient related to the cloud physics of the storm cloud water droplets and b is another empirical co-efficient related to the type of storm cloud present. This relationship has proven to produce highly variable results. Since the values of both A and b are variables that must be assumed, opportunities for errors in the calculation are possible.

The algorithms used to estimate the rainfall are standard for use around the country and have not proven to be responsive to local cloud variations. The r-squared or "goodness" of the rain to radar reflectivity statistical relationship has varied from 0.15 to 0.90 on a daily basis and for most storm seasons has been about 0.60.

The good r's (values >0.75) have been for the low volume and low intensity rain events (stratiform rainfall), generally those of less than 0.25"/hr accumulation rates. The high intensity, high volume, thunderstorms (convective rainfall) have shown r-values of 0.15 to 0.45. Thus the standard products appear to be unreliable at this point. The storm rainfall has been both overestimated and underestimated for periods of less than three hours for storms within 25 miles of each other.

Finally, hail "contamination" of the equation has proven to be a troublesome problem to deal with as well. Since the strength of the radar signal is related objectively by the algorithm to the estimated rainfall, the strong radar return value of hailstones will usually cause an over-estimation of the rainfall rate.

HMS uses its own method to solve these problems related to rainfall over and under estimation. The HMS method uses the radar reflectivity to locate the portion of the precipitating cloud where the heaviest rainfall is located rather than to calculate a rainfall rate. In over 90 percent of the operational heavy rain days in the Urban Drainage & Flood Control District since 1985, HMS has observed that the heaviest rainfall has occurred when the strongest radar reflectivity field passes over the rain gauges. Given the validity of this assumption, the next step is to calculate the peak rainfall rate associated with the storm, which can in turn be related to the strongest radar reflectivity values.

Since late 1981, HMS has used a combination of surface weather station data and a 2-D cloud methodology to predict the peak rainfall rate associated with convective rainfall. HMS has found that the depth of a thunderstorm's updraft that is warmer than 0° Celsius is directly related to the rain-production potential of the cloud. When the warm depth of the updraft exceeds 1.5 km in Colorado, for instance, the rain-production potential of the cloud doubles.

Equation (2) shows a simplified form of this relationship:

- (2) **Peak 60-minute rainfall =**
PWI X (Depth of updraft warm layer) X 2 1.5km
- (3) **Peak 30-minute rainfall = 0.70 X (Peak 60-min rain)**
- (4) **Peak 10-minute rainfall = 0.60 X (Peak 30-min rain)**

Where the Precipitable Water Index (PWI) is a measure of the amount of water in the atmosphere from the surface to about 20,000 feet above the ground. HMS generates a matrix of rainfall rates, which are derived from surface temperature and dew point fields used to initialize the 2-D model output. For each set of surface temperature-dew point combinations, HMS creates a unique radar-rainfall relationship for precipitation mapping. In effect the peak 60-, 30-, and 10- minute rainfall rates are related to the 50 dBZ or greater radar reflectivity values within the thunderstorm. Lower rain rates are logarithmically down-stepped to the lower radar reflectivity values.

3.3 Saguache Creek Basin Rainfall Estimation Methodology

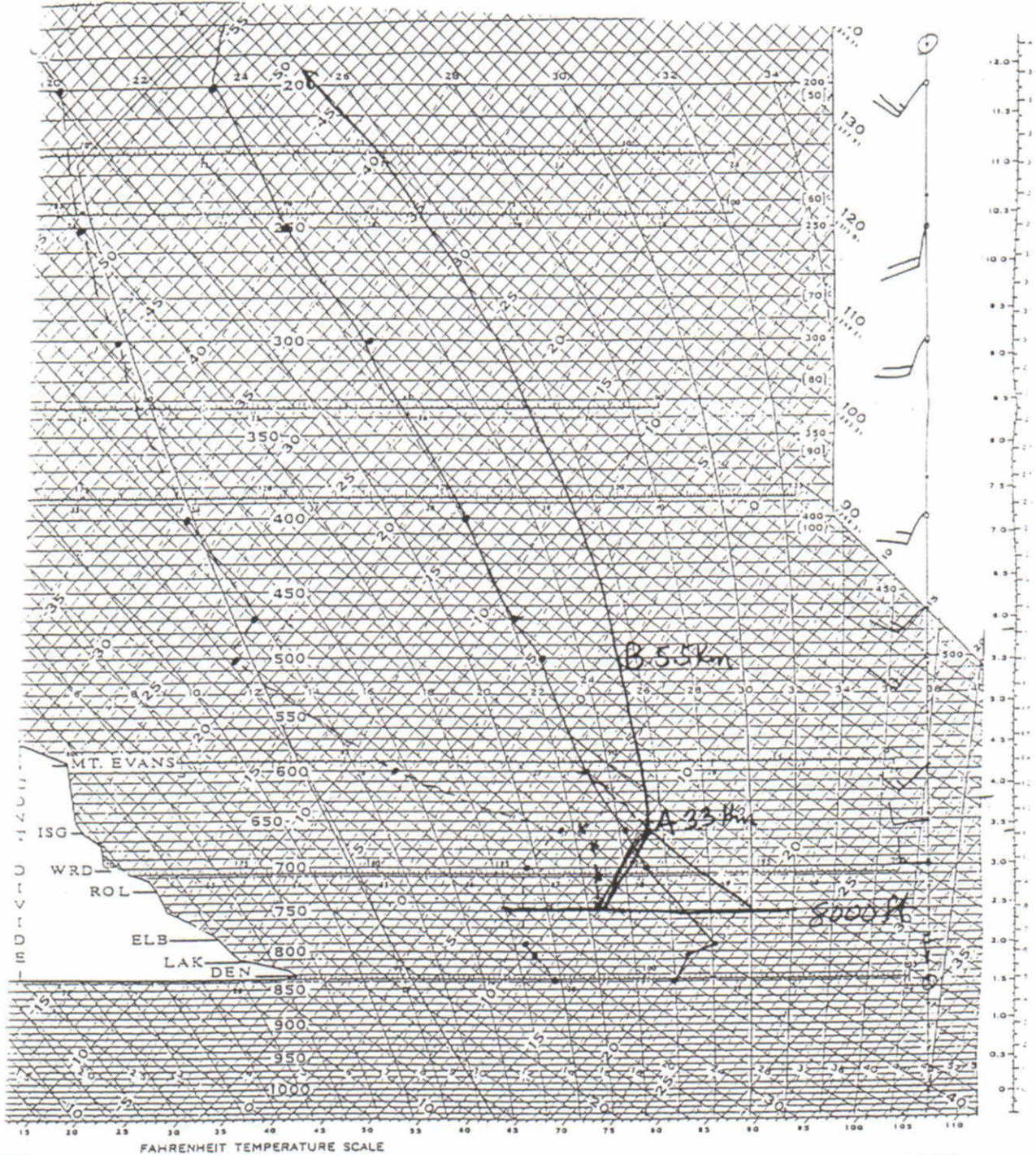
Nearby METAR weather stations temperature/dew point values were used to initialize the HMS 2-D cloud model for rainfall estimation. For the event of July 25th, 1999 near Saguache, Colorado HMS utilized METAR observations at Leadville, Alamosa, Gunnison and Montrose Colorado to calculate and assign a radar-rainfall relationship to the outlined basin (**Table 1**).

Station	Temperature (F)	Dew point (F)
Montrose	80	57
Alamosa	74	52
Gunnison	73	48
Leadville	67	42

Table 1
Surface Observations for Nearby Stations of Saguache, Co.
At 1900 UTC (1 P.M. Local) July 25,1999.

An example of this relationship and the calculations for the afternoon of July 25, 1999 will now be discussed to illustrate the points just made. HMS plotted the above-mentioned METAR observations on a Skew-T, Log P diagram, containing information derived from a radiosonde, launched at Grand Junction Colorado, to calculate the PWI. **Figure 5** shows the HMS-plotted Skew-T, Log P diagram for the afternoon of July 25th where point A is the cloud base and point B is the point where the thunderstorm updraft cools to 0° C. The calculated PWI is 1.16" adjusted for an elevation of 8,500 feet while the depth of the warm updraft layer is point B (5.5 km) minus point A (3.3 km) or 2.2 km. The next step is to solve equations (2) and (3) to calculate peak rainfall rates.

Figure 5
Modified Albuquerque Sounding for Saguache Creek Flood



STATION: ABQ
 NUMBER: _____
 TIME (GCT): 12Z
 DATE (GCT): 7-25-99

PRECIPITABLE WATER		
LYR	MR	CONV PWI
820	_____	0.044 _____
750	_____	0.133 _____
650	_____	0.154 _____
555	_____	0.182 _____
TOTAL:	_____	13.2 = -96"

ME50 = 1.16"

STABILITY DATA					QPF		
T	Td	DelT	DelZ	PF	60 min.	30 min.	10 min.
1.	_____	_____	_____	_____	_____	_____	_____
2.	_____	_____	_____	_____	_____	_____	_____
3.	_____	_____	_____	_____	_____	_____	_____
4.	_____	_____	_____	_____	_____	_____	_____
5.	_____	_____	_____	_____	_____	_____	_____

If you insert the values for PWI and the depth of the warm layer into equations (2) and (3), the peak 60-minute rainfall rate is 3.42" and the peak 30-minute rainfall rate is 2.38 inches. These rainfall rates are assigned to the grid squares covered by radar reflectivity values of 50 dBZ or greater. Lower rainfall rates are assigned to lower reflectivity values as shown in **Table 2**.

Radar dBZ - Level	Peak 60-min	Peak 30-min
25		
30	0.72"	0.50
35	1.20"	0.85
40	1.92"	1.34
45	2.40"	1.68
50	3.36"	2.38"
55	3.36"	2.38"

Table 2
Relationship Between Peak 60-Minute and Peak 30-Minute Rainfall Rates and Radar Reflectivity Levels.

HMS utilized the Doppler radar from the National Weather Service (NWS) WSR-88D located at Pueblo, Colorado. This radar is located about ~115 miles from the basin and provides fairly accurate radar reflectivity observations. HMS notes that the Pueblo is slightly affected by the passage of its beam over higher terrain to the west. HMS estimates that up to 30% of the lower half of the beam may be attenuated as it shoots towards the Saguache location along a 255-degree radial. However, this factor matters little as HMS does not use the absolute strength of the radar reflectivity to calculate the rainfall rates but rather uses the strength of the maximum reflectivity to identify the location of the heaviest rainfall. The rate is calculated by the HMS 2-D cloud model.

As the radar reflectivity data field is received and mapped; each grid square is assigned a reflectivity value of 0 through 7. **Table 2** above shows the reflectivity values and their associated dBZ values.

3.4 Analysis of Radar Reflectivity and Rainfall

This section will encompass an examination of the radar reflectivity pattern and the rainfall pattern that accompanies it. The resolution of the radar reflectivity data allows it to define the radar reflectivity for 0.65 by 0.65 square mile area. **Figure 6** shows a summation of the reflectivity value for each grid square for the duration of the storm. Note that a rainfall rate (See **Table 3**) is assigned to each radar reflectivity factor for each observation and the storm total rainfall is a summation of these individual rainfall observations. Note that the grid is segmented into an outer and inner grid and that the inner grid is split along the stream location of the valley of the basin.

3	5	12	10	12	11	9	10	12	13	13	18	21	20	18	14	13	17	19	22	20
3	4	10	9	9	9	8	8	8	14	17	20	30	27	26	23	23	27	29	30	25
1	2	6	9	8	8	9	8	16	20	22	27	32	33	32	30	26	24	29	27	27
0	1	0	2	3	6	12	12	18	21	29	30	35	40	35	37	30	30	35	36	34
0	1	0	2	3	7	11	11	24	27	30	35	35	44	36	41	36	39	41	47	40
0	0	0	0	0	6	14	18	35	38	50	53	48	47	40	46	47	48	44	46	42
0	0	0	1	1	8	18	26	44	50	55	56	53	50	53	55	55	54	49	51	45
0	0	2	1	1	7	24	34	54	60	64	58	54	54	52	54	58	58	51	51	51
0	0	2	2	3	9	31	42	60	66	69	64	62	68	64	64	64	65	51	53	45
0	0	2	2	10	21	43	54	71	78	74	64	62	64	62	67	68	60	55	51	46
1	1	4	5	14	25	44	57	72	81	81	78	68	68	61	59	61	60	58	54	44
0	1	1	3	5	17	33	46	62	73	81	81	77	75	62	61	64	55	48	43	42
0	1	1	5	5	16	33	50	62	76	82	78	74	71	61	62	62	62	56	49	47
1	4	3	5	7	14	32	47	62	71	74	72	65	63	66	62	58	61	58	53	54
5	6	4	5	7	13	31	44	58	66	60	61	59	61	64	61	56	56	51	43	45
5	6	4	5	8	12	30	41	52	60	55	54	54	53	52	50	51	54	50	50	50
7	7	5	6	10	15	26	34	37	45	46	47	46	49	51	53	52	50	47	44	45
7	7	9	10	9	10	12	24	31	37	44	42	40	42	46	46	49	48	44	42	35
3	6	8	8	10	11	13	20	26	30	28	31	33	41	38	37	37	36	35	32	31
3	7	8	10	12	10	12	15	20	25	26	24	26	29	26	25	26	29	26	25	25
3	7	8	10	10	10	11	7	13	16	18	22	23	25	20	23	24	25	23	23	21

Figure 6
Shows the Summed Radar Reflectivity Levels for Each Grid Square

Radar reflectivity values (dBZ)	5-min rainfall rate	Radar reflectivity levels
<30	0	0
30	0	1
35	0.05"	2
40	0.10"	3
45	0.15"	4
50	0.20"	5
55	0.28"	6
>55	0.28"	7

Table 3
Relationship Between Radar Reflectivity Values (dBZ)
and HMS Derived Radar Reflectivity Levels

Figure 7 shows the HMS radar-estimated storm rainfall from 1428 MDT until 1642 MDT across the basin based on the technique described above. The basin average rainfall during this period was 3.50 inches of rain with a peak 0.65 square mile rainfall of 5.20 inches. The peak square mile rainfall was 4.99 inches. Note that the storm has formed a rather symmetric pattern with lobes of heavy rainfall extending to the northeast and southeast. The radar pattern indicated that two storm complexes moves within the pattern with first one moving from southwest to northeast and the second one moving from northwest to southeast. This change in cell direction suggests that a disturbance moved across the area affecting the movement of the cells.

0.10	0.10	0.25	0.20	0.30	0.15	0.20	0.20	0.10	0.10	0.10	0.31	0.47	0.42	0.26	0.16	0.75	0.92	1.20	1.14	0.96
0.10	0.10	0.20	0.20	0.25	0.20	0.20	0.15	0.05	0.25	0.31	0.58	0.78	0.85	0.79	0.86	1.19	1.31	1.37	1.26	0.97
0.00	0.00	0.15	0.20	0.20	0.20	0.15	0.15	0.30	0.35	0.30	0.66	0.88	0.95	1.13	1.07	1.14	1.09	1.37	1.21	1.08
0.00	0.00	0.00	0.00	0.05	0.10	0.20	0.25	0.35	0.35	0.77	0.93	1.20	1.54	1.40	1.40	1.19	1.57	1.91	1.90	1.60
0.00	0.00	0.00	0.00	0.05	0.10	0.20	0.20	0.72	0.94	0.83	1.31	1.15	2.03	1.67	1.78	1.41	1.92	2.49	2.82	2.19
0.00	0.00	0.00	0.00	0.00	0.05	0.20	0.40	1.39	1.46	2.18	2.62	2.20	2.32	2.12	2.34	2.35	2.91	2.76	2.64	2.41
0.00	0.00	0.00	0.00	0.00	0.05	0.20	0.73	2.08	2.48	2.50	2.78	2.49	2.48	3.07	3.24	3.12	3.21	3.00	2.97	2.59
0.00	0.00	0.16	0.00	0.00	0.05	0.68	1.20	2.82	3.16	3.29	2.96	2.68	2.78	3.09	3.32	3.30	3.37	3.11	2.98	3.02
0.00	0.00	0.16	0.00	0.16	0.21	1.23	1.81	3.27	3.67	3.80	3.61	3.46	4.21	4.12	4.30	3.91	3.98	3.18	3.18	2.92
0.00	0.00	0.16	0.00	0.48	0.85	2.38	3.00	4.18	4.61	4.40	4.15	4.03	4.13	4.30	4.46	4.22	3.60	3.22	2.95	2.78
0.00	0.00	0.16	0.16	0.80	1.29	2.49	3.17	4.19	4.91	5.08	4.97	4.27	4.62	4.15	4.13	3.94	3.79	3.53	3.35	2.96
0.00	0.00	0.00	0.00	0.16	1.02	1.83	2.74	3.64	4.43	4.96	5.08	4.90	5.03	4.31	4.33	4.40	3.75	3.11	2.84	2.82
0.00	0.00	0.00	0.16	0.16	1.02	1.90	3.13	3.92	4.89	5.20	4.91	4.74	4.76	4.57	4.60	4.38	4.32	3.71	3.16	3.15
0.00	0.16	0.00	0.16	0.32	1.02	2.13	3.15	3.99	4.57	4.72	4.71	4.33	4.33	4.87	4.61	4.26	4.21	3.96	3.33	3.47
0.38	0.38	0.16	0.16	0.16	0.86	2.07	2.93	3.87	4.40	3.94	4.09	4.17	4.23	4.64	4.38	3.98	3.92	3.51	2.73	2.75
0.38	0.38	0.16	0.16	0.32	0.80	2.07	2.88	3.55	4.00	3.67	3.56	3.71	3.55	3.66	3.67	3.35	3.51	3.15	3.09	2.96
0.54	0.54	0.32	0.22	0.54	0.96	1.90	2.43	2.66	2.92	2.99	3.11	2.94	3.27	3.58	3.62	3.67	3.31	3.10	2.65	2.81
0.54	0.54	0.54	0.60	0.70	0.60	0.86	1.78	2.17	2.58	2.92	2.76	2.40	2.54	3.13	3.11	3.45	3.14	2.60	2.57	1.97
0.16	0.48	0.54	0.38	0.70	0.76	0.92	1.46	1.67	2.02	1.86	1.92	1.92	2.41	2.47	2.33	2.51	2.27	2.03	1.92	1.86
0.16	0.54	0.54	0.54	0.86	0.60	0.76	1.08	1.14	1.58	1.79	1.42	1.37	1.57	1.63	1.42	1.60	1.88	1.31	1.36	1.31
0.16	0.54	0.54	0.54	0.64	0.60	0.76	0.44	0.60	0.92	1.20	1.36	1.09	1.40	1.02	1.22	1.50	1.48	1.38	1.32	0.97

Figure 7
Shows Total Rainfall for Each Grid Square

The estimated volume of the rainfall was approximately 13,242 acre-feet of water and it fell over a roughly 8 mile by 8-mile volume covered by the storm's 1-inch or greater coverage area. It is little wonder that flooding occurred given the volume of rain.

Figure 8 shows the time and intensity distribution of the storm for the basin average rainfall and the eastern and western portions of the sub-grid where the heavy rainfall occurred. **Note that over 90% of the rain fell in just less than two hours though the entire storm lasted three hours.** The west basin rainfall maximum preceded the east basin's maximum by about 20 minutes while the maximum value of the east basins rainfall was slightly larger.

The storm rainfall began over the basin at approximately 228PMMDT and lasted until 524PMMDT. The peak rainfall in the west basin occurred from 330PM MDT to 345PM MDT while the east basin peaked from 405PM to 440PM in a singular and longer peak.

4.0 Cloud to Ground Lightning Data

In order to better examine this particular event, Cloud to Ground Lightning Data (CG) was analyzed in with respect to both the topography and the reflectivity/rainfall pattern. CG data was acquired from the National Weather Service's (NWS) National Lightning Detection Network (NLDN) through its contract operator, Global Atmospheric, Inc. (GAI). HMS obtained CG data for a 24-hour period for a circular area with a 25-mile radius centered on the affected flooded area near Saguache. The CG data was then parsed according to whether or not it struck within, or very near, the grid area defined in the rainfall estimation section. (See **Figure 9**)

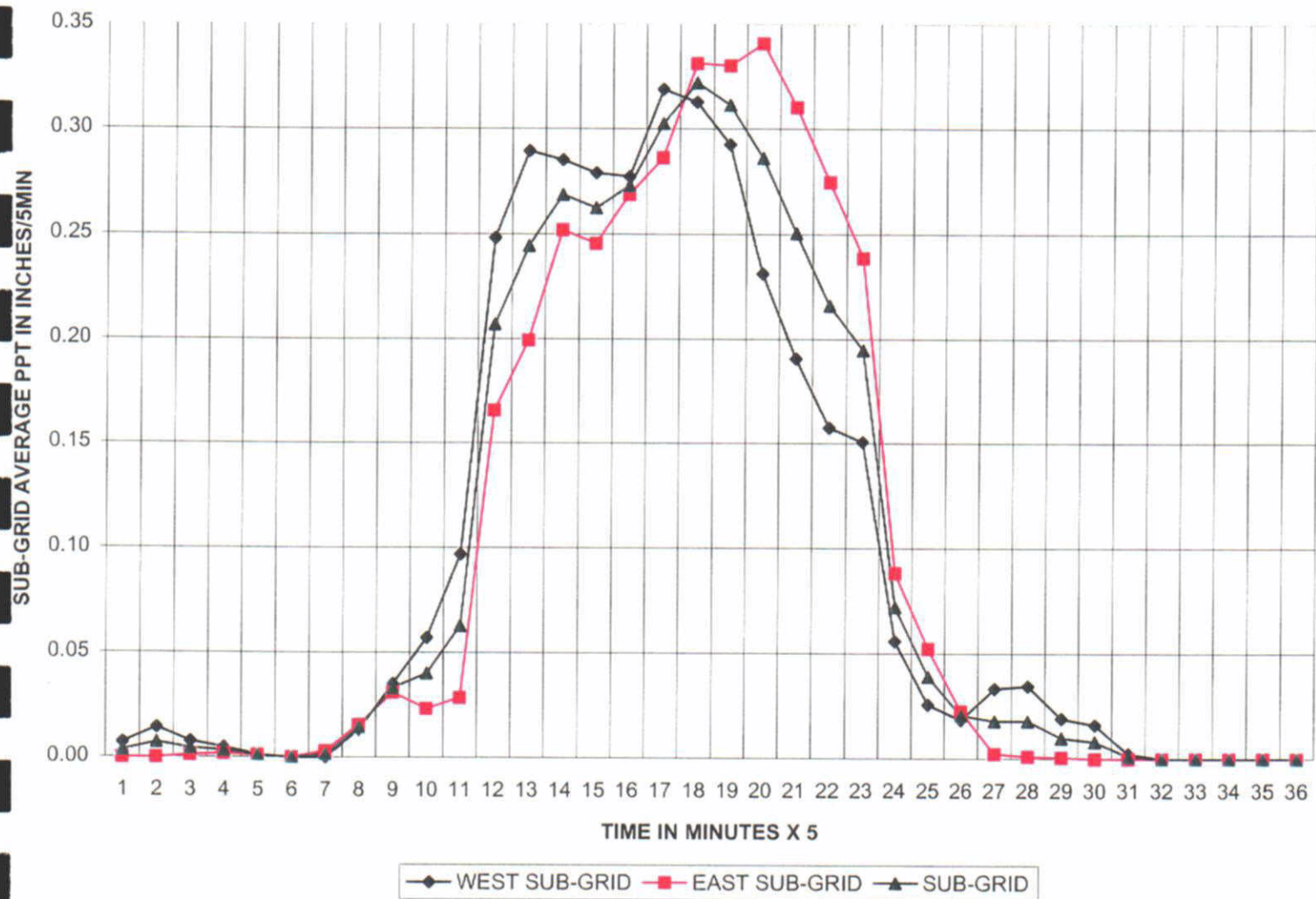
The data was re-plotted, using the latitude and longitude of each CG strike, for 15-minute segments starting at 2115 UTC (3:15 PM MDT) and ending at 2245 UTC (4:45 PM MDT) for the grid area, which can be seen in the Appendix. The grid located CG data was divided up into 5-minute segments corresponding with the radar reflectivity images available. A total of 274 CG strikes were detected in or near the grid for the entire duration of the event. The distribution of the CG strikes was separated into 5-minute segments and the temporal distribution for these strokes in the grid. The peak 5-minute count of grid-based CG strokes (34) occurs in the time interval from 2204UTC to 2209UTC (4:04 to 4:09 PM MDT).

4.1 CG Data and Topography

Spatial-temporal analyses of the CG lightning data with respect to geography and topography were also made to study any possible impact topography made have had in the CG distribution. Comparisons of the grid topography and CG strike locations show that in the first 15 minute period of notable lightning activity (2130-2145 UTC), that over half of the strikes were on the east side of the Middle Creek valley while other strikes were fairly scattered in nature. These strokes also did not show any particular favor towards the elevation at which they struck.

Figure 8
Temporal Rainfall Distribution of
the Saguache Flood in Analysis Grid

SAGUACHE SUB-GRID AVERAGE PPT VS TIME 2028-2324 GMT JULY 25, 1999



The following 15-minute period (2145-2200 UTC) continues to show vigorous CG activity focused on the Middle Creek valley with a vast majority of the strikes occurring between 9000' and 10000' in elevation. The next period (2200-2215 UTC), continues to show a high number of CG strokes in and along the Middle Creek valley, with nearly a quarter of the 88 strikes in this period striking along the sides of Baxter Mountain, which is in the upper portion of the Middle Creek basin.

Once again, nearly all strikes (75/88) were at elevations above 9000'. Between 2215-2230 UTC, just over 50% of the 65 CG strikes during the period, were confined to a relatively small area in the central portions of Bear and Cross Creeks with nearly all of the strikes, once again, occurring between 9000' and 10000'. All other strikes during this period were relatively scattered in nature. As the core of the storm moved primarily to the southeast of the grid area 17 of 37 CG strikes that occurred were clustered in the lower portions of Cross and Middle Creeks below 9000' with all other strikes either scattered, or out of, the immediate area of interest.

4.2 CG Data and Radar Reflectivity

Further analysis on the relationship between radar reflectivity and the CG lightning data was also performed. In the 2115-2130 UTC period only 2 strikes occurred in the grid however, during this brief period the storm experienced a notable increase in the intensity of the storms maximum reflectivity to the 50+ dBZ level. From 2130-2145 UTC, a majority of CG strikes in this period appear to occur in the area surrounding the 50+ dBZ level in the core of the storm. In the period from 2145 to 2200 UTC, an argument could be made that there are two distinct patterns to the CG strokes.

The first is the appearance that a fair number of strokes (27 of 58) are close to the edge of the 30 dBZ boundaries at either 2149 or 2154 UTC. A second pattern, albeit not as conclusive, is that a secondary group of strokes appear to be near the 50+ dBZ core at some point in this segment. In addition, these patterns show that the CG strokes were located primarily to the north, which is to the left of the mean wind steering flow.

During the 2200-2215 UTC period, which contains the most CG activity, the majority of the strikes were well to the north of the storms 50+ dBZ core but the strikes do not appear to 'hug' the 30+ dBZ area as closely as at other time periods. In addition, there were a minimal number of strokes (4) that were in the proximity of the 50+ dBZ area. From 2215-2230 UTC, the pattern of CG strikes appears to support the occurrence of strikes on the edges of both the 30+ and 50+ dBZ areas. However, as the storm core leaves the grid area, the strikes appear to be located on the west and northwestern edges of these areas.

The final period (2230-2245 UTC) of the grid-based CG data shows that strokes continue to occur even though the vigorous area of the storm (+50dBZ)

is no longer present in the grid. A quick examination of this period shows that some of the strokes do appear to be on the edge of the 30+ dBZ areas however, the orientation of the strikes with respect to the reflectivity pattern does not appear to have a discernable pattern due to the scattered nature of the radar reflectivity at this time.

4.3 CG Data and Grid Averaged Rainfall Rates

A comparison of the grid averaged rainfall and CG rates for 5 minute intervals is shown in **Figure 10** for the entire analysis grid while **Figure 11** shows the same rate for the sub-grid area where the heaviest rain fell. . The grid averaged rainfall rate was simply derived by averaging the derived 5-minute rainfall rates over the grid of the area.

A brief glance at these two graphs shows that the timing of the increases, peaks, and decreases in average rainfall vs. CG lightning indicate that **the peak rainfall rate precedes the corresponding CG intensity by 5-10 minutes**. When the CG and rainfall data is further broken down into a sub-grid area that is roughly defined as > 3.00" storm total rainfall, the lag in the near area CG stroke counts with respect to the sub-grid averaged rainfall rates is increased to **about 10-15 minutes (Figure 11)**. This pattern is suggestive of the existence of a warm coalescence rainfall mechanism operating. Warm coalescence rainfall periods usually produce the heaviest rainfalls and rainfall rates and low lightning rates frequently appear during the periods of heaviest rainfall during flooding events.

5.0 Relationship of Rainfall to Topography

A constant source of debate concerning the rainfall limits of heavy rain has existed since the mid-1980s. **Table 4** shows the average and range of rainfall rates for the storm versus elevation. Note that the heaviest rainfall fell between 8,000 feet and 9,000 feet in the valley with over 4.00 inches of average rainfall. It is interesting that for every 1,000 feet of elevation increase the base rainfall decreases about 25 percent. If this relationship holds up in other storms, it could have a profound impact on the calculation of elevation adjustments to site specific Probable Maximum Precipitation (PMP) calculations.

Elevation Band	Rainfall Range	Average Rainfall	% reduction
Above 10,000 feet	1.75"-2.05"	1.85"	-57%
9,000 – 10,000 feet	2.00" – 4.50"	3.25"	-25%
8,000 – 9,000 feet	3.00 – 5.00"	4.35"	0

Table 4
Relationship of Rainfall Amount to Elevation

Figure 10
 Temporal Distribution of C-G Lightning Compared to Basin and Average Rainfall

SAGUACHE GRID AVERAGE PPT/C-G LIGHTNING/5 MIN JULY 25, 1999

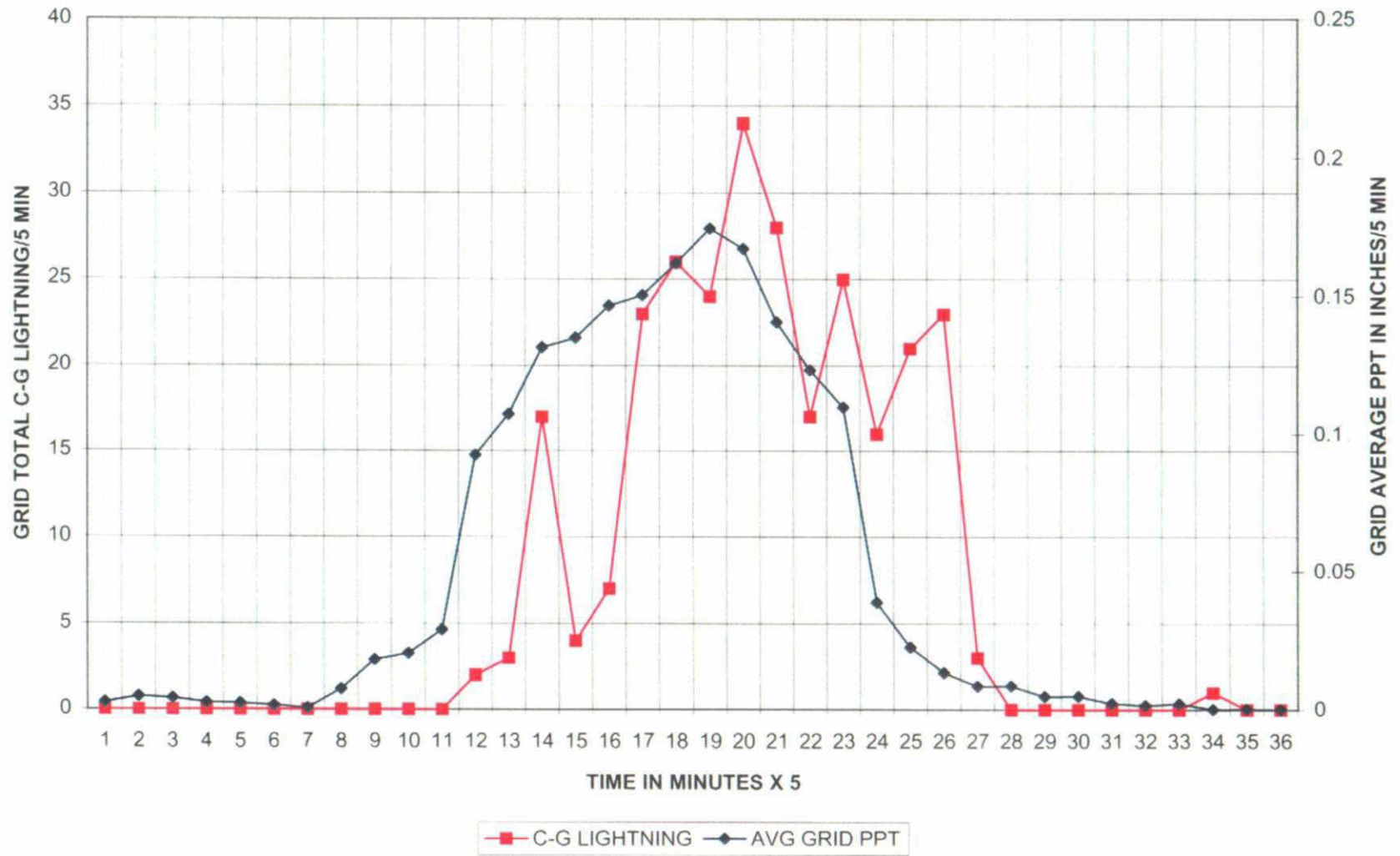
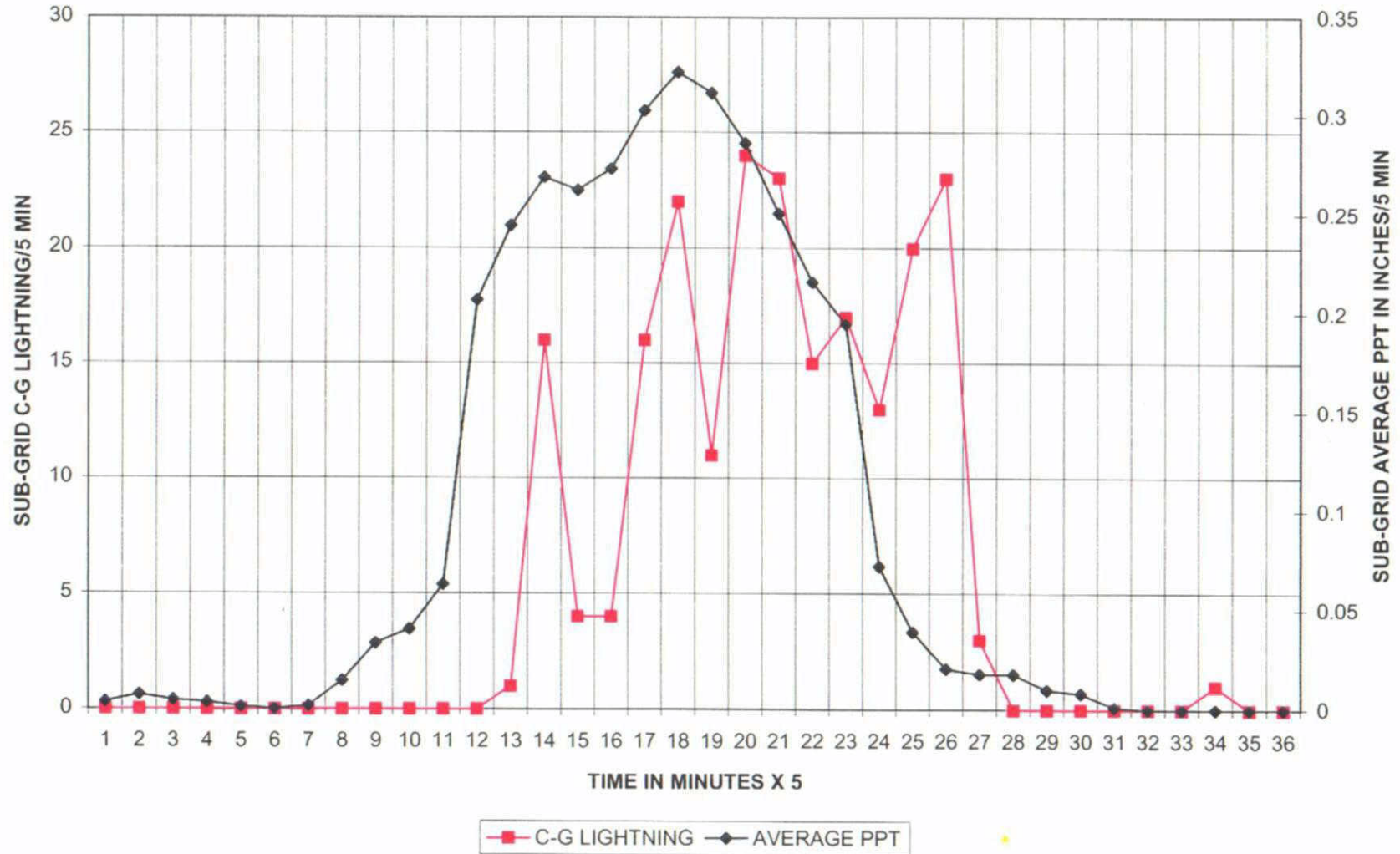


Figure 11
 Temporal Distribution of C-G Lightning Compared to Basin and Average Rainfall

SAGUACHE SUB-GRID C-G LIGHTNING/ PPT VS. TIME 2028-2324 GMT JULY 25, 1999



6.0 Comparison of Paleo-Hydrologic Derived Storm and Radar Rainfalls

Bob Jarrett of the USGS performed a preliminary estimate of the run-off derived rainfall based on a field survey of the flood damage fields in the floodplains. **Figure 12** shows the Jarrett isohyetal pattern developed by "backing into" the rainfall by estimating the runoff for the Saguache flash flood. Jarrett used time honored run-off estimation techniques based on observed high-water marks, flood debris and floodplain scarring caused by the runoff.

After gathering this evidence, he calculated the area and volumes affected by the flood, noted high water marks and estimated runoff. From the runoff values he estimated the precipitation necessary to produce the evidence he collected and from multiple locations he creates the isohyetal pattern observed. This simple description does not do justice to the techniques and painstaking labor of science and love he applies.

Figure 13 shows the Jarrett rainfall pattern overlain by the radar-derived rainfall pattern in one-inch increments. Note the following similarities and differences in the two patterns:

- First, the radar-derived pattern covers roughly twice the area of the runoff derived precipitation pattern. However, the radar-derived 4-inch isohyets covers roughly the same area as the entire run-off derived pattern.
- The peak runoff derived rainfall is over 6 inches while the radar-derived value is just over 5 inches. Strangely, the run-off derived precipitation area covered by 5 inches or more of rain is roughly twice the size of the radar derived 5-inch area and anchored further east in the region of tightest elevation gradient.
- Note that both patterns show a roughly east-west axis of the heaviest rainfall and the southeastward extending lobes of heavier rainfall.

The possible reasons for these discrepancies will not be discussed in this paper but it is heartening to see the many similarities in the two patterns. Additional patterns will be compared and possibly assist in providing a key to using the runoff derived technique effectively in paleo-hydrologic studies for eras in which no radar data exists.

7.0 Conclusions

A flash flood occurred over the higher terrain roughly 5-10 miles northwest of the small town of Saguache, Colorado during the afternoon of July 25, 1999. The meteorological causes of the flash flood were related to the passage of a monsoon weather disturbance identified on satellite and associated with a very moist area of mid-level air from 10,000 to 20,000 feet.

Figure 12
 Jarrett Runoff Derived (RO) Rainfall Pattern for Saguache Flood

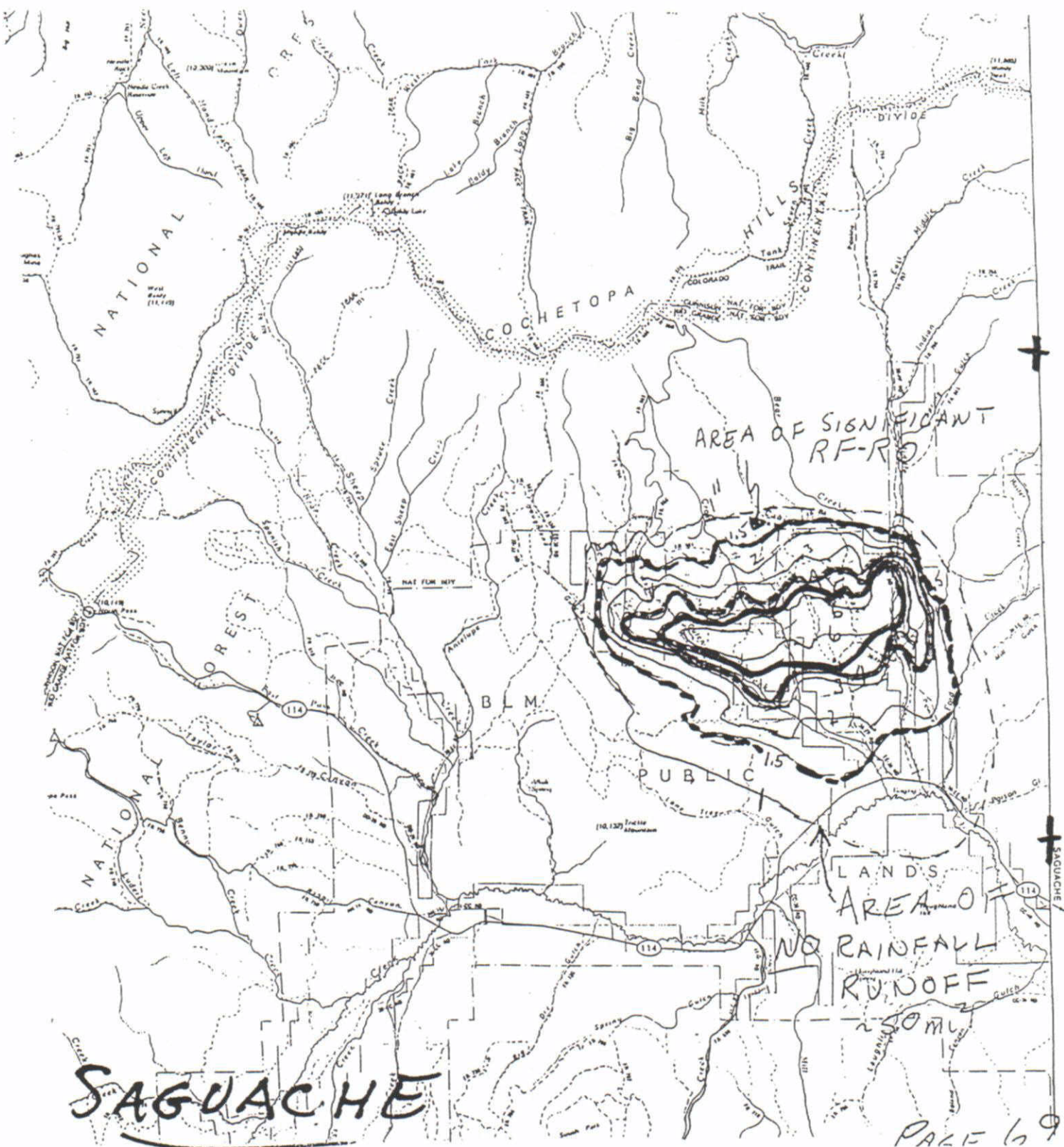
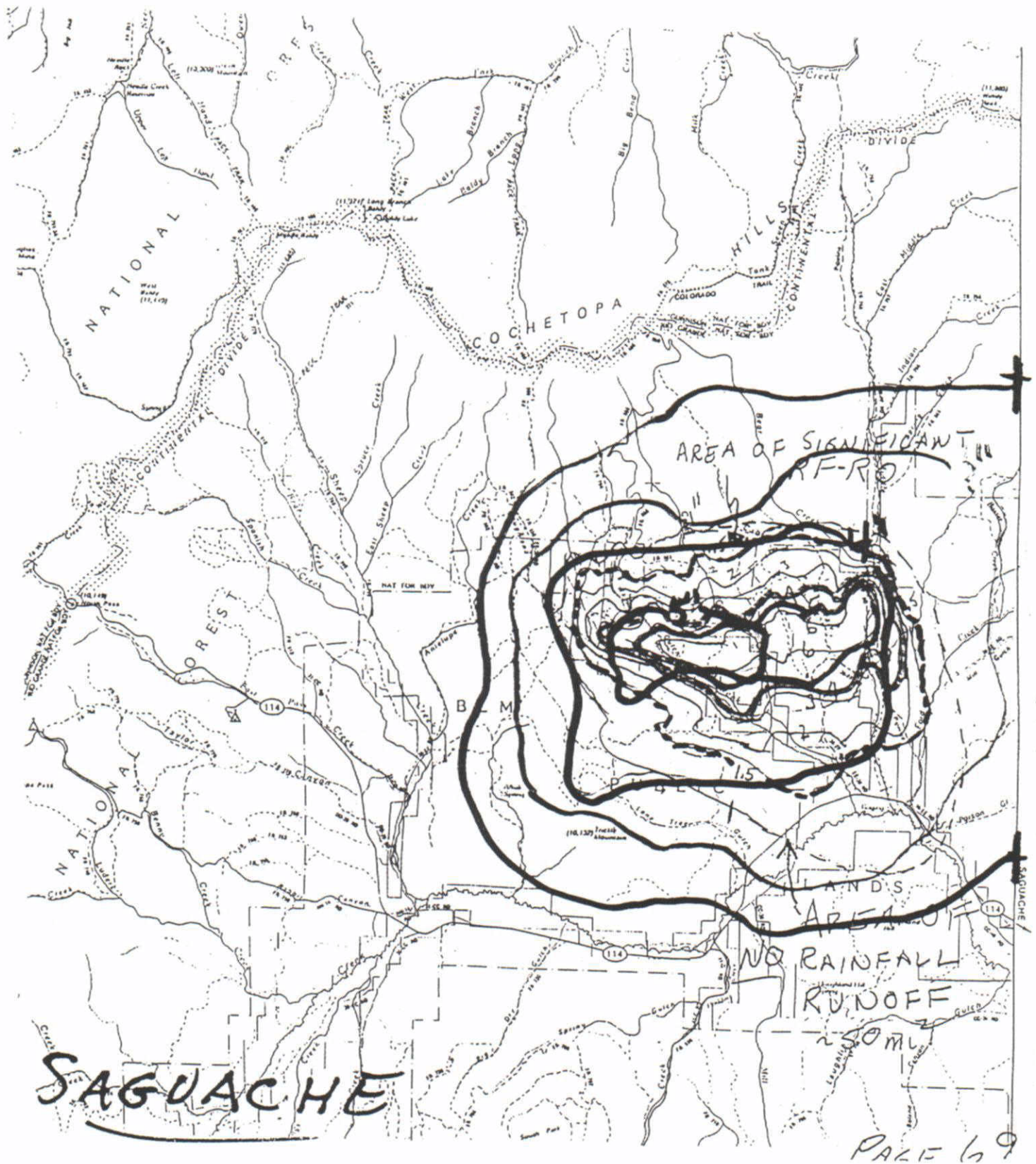


Figure 13
Sub-Grid Jarrett Runoff Derived (RO) Rainfall Pattern for
Saguache Flood Overlain by the Radar-Derived (RD) Rainfall Pattern



Daytime heating of the local topography initiated the development of the storms. The storm began raining in the basin about 300PM MDT, reached its peak rain production between 330PM MDT and 430PM MDT and moved off the basin and dissipated between 500PM MDT and 600PM MDT. The duration of the peak rainfall was about two hours.

The storms were "locked" into the terrain by slow moving winds that flowed in the cloud layer directly into an area of steep elevation gradient as new cells developed over a small mountain immediately to the west of the basin. The axis of the heaviest rainfall was along the mean winds in the 10,000 to 20,000 foot layer of the atmosphere. The heaviest rainfall area was located over the middle of the basin at elevations below 10,000 feet. The average elevation of the 5.00-inch isohyetal was about 8,750 feet.

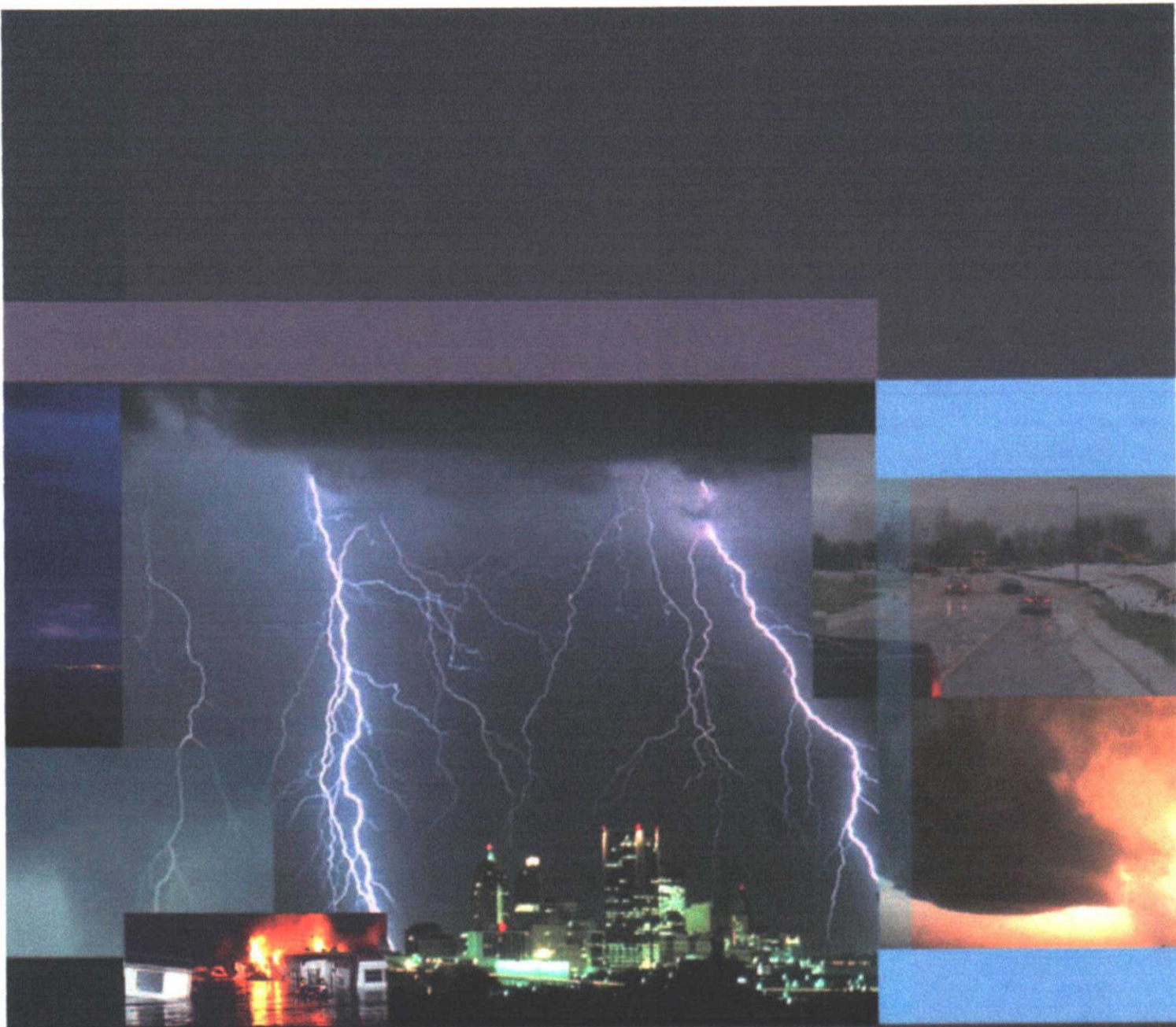
The storm produced peak radar derived rainfall of just over 5 inches at elevations of 8,000 to 9,000 feet and produced rainfalls exceeding 4.00 inches in elevations to almost 10,000 feet. This rainfall is among the largest estimated at such high elevations in the Colorado Mountains.

The storm covered an area of roughly 72 square miles with a basin average rainfall of 1.84 inches in this area. A smaller area of average rainfall of 3.50 inches covered an area of roughly 30 square miles.

Cloud-to-ground lighting production of the storm produced several interesting observations. First, the peak lightning areas hugged the terrain gradient areas to the north and to the east of the storm rainfall area with over 80 percent of the cloud-to-ground lightning strikes in the 9,000 to 10,000 foot elevation band. Most of these strikes were to the north of the heaviest rainfall area in an area of decreasing radar reflectivity gradient,

A casual comparison of the radar-derived (RD) and run-off derived (RO) rainfall patterns showed the RD areas of 2.00 inches or more rainfall as roughly twice as large as the comparable RO area but the RO area of heaviest rainfall was about twice the RD heavy rainfall area of 5.00 inches of rain or more. In general, the two rainfall estimates identified the same areas of the basin impacted by the flooding. A more quantitative comparison of these differences begs to be accomplished.

In closing the rainfall values presented in this study should be of assistance in providing an estimated but quantitative description of the storm. The advent of radar coverage by National Weather Service WSR-88D Doppler radars allows reasonable estimates of the spatial and temporal characteristics of heavy rain producing thunderstorms across the Colorado Mountains. Additionally, the radar observations afford the opportunity to provide quantitative estimates of the amount and volume of rainfall.



HDR